A Frequency-Dependent FDTD Method for Biological Applications

Dennis M. Sullivan, *Member, IEEE*

Abstract—**A frequency-dependent finite difference time domain (FD)^{2}TD method to calculate the response of pulses in plasma or water has recently been described. This method is an advance over the traditional finite-difference time-domain (FDTD) method in that it allows for the frequency dependence of these two media. In this paper, the (FD)^{2}TD method has been modified to obtain broad band frequency information in 3-D biological applications. The implementation of this method is described and its accuracy is verified by comparison with analytic solutions using the Bessel function expansion. The use of this method is illustrated by an example of the 3-D simulation of a hyperthermia treatment using two-applicators over a frequency range of 40 to 200 MHz.**

I. Introduction

THE FINITE-difference time-domain (FDTD) [1] method has proven to be an effective method of calculating the interaction of electromagnetic (EM) waves with bodies of different shape and different material. It is particularly effective in the calculation of large three dimensional structures because, for a given cell size, computation and storage requirements increase only linearly with the number of cells [2]. It has seen extensive use in military applications where it is often used to calculate the scattering from a metallic surface [3]–[5], in electromagnetic dosimetry where the specific absorption rate (SAR) is calculated in a body exposed to EM radiation [6]–[7], and more recently, in hyperthermia cancer therapy [8]. In hyperthermia applications, it has been used in the design of radio frequency (RF) and microwave applicators, and for simulation of treatment on commercially available applicators [9]. For the latter application, it has recently been put into clinical use [10].

For the dosimetry and hyperthermia applications, one is generally interested in the SAR distribution within a biological body for one or more sources at a given single frequency. However, it is often desirable to have the results at several different frequencies, to determine the frequencies which are most hazardous, in the case of EM dosimetry, or to find the frequency which is most effective for hyperthermia. A method has been described which obtains multiple frequency information with one computer run [10], [11], but this has been of questionable use in biological applications because of the frequency dependent characteristics of biological tissue.

Recently, an implementation of the FDTD method which allows for the frequency dependence of dielectric properties has been described by Luebbers, *et al.* [12], [13]. The authors refer to it as the frequency-dependent finite-difference time-domain (FD)^{2}TD method. This method was demonstrated by calculating wide band pulse reflections from water [12] and from plasma [13]. In the present paper, the implementation of this method into three dimensional biological applications for the purpose of obtaining SAR distributions for multiple frequencies with one run is described. In section II of this paper, it will be shown that the implementation of this new method requires only a simple extension of the previous formulation of the FDTD method for EM dosimetry and hyperthermia [6], [7], [9], [10]. Section III describes the determination of input parameters for this method. In Section IV, the accuracy of this method is evaluated by comparison with analytic solutions using a Bessel function expansion technique. Section V is an example of the applicability of the (FD)^{2}TD method for hyperthermia simulations.

II. Description of the Method

Starting with the Maxwell equations:

$$j\omega \boldsymbol{D}(\omega) = \nabla \times \boldsymbol{H}(\omega) - \boldsymbol{J}(\omega) \tag{1a}$$

$$-j\omega \boldsymbol{B}(\omega) = \nabla \times \boldsymbol{E}(\omega) \tag{1b}$$

and the relationship between the electric flux density and the electric field in the frequency domain

$$\boldsymbol{D}(\omega) = \epsilon_0 \cdot \epsilon(\omega) \cdot \boldsymbol{E}(\omega) \tag{2}$$

the complex dielectric constant $\epsilon(\omega)$ is given by

$$\epsilon(\omega) = \epsilon_\infty + \chi(\omega) \tag{3}$$

and the susceptibility $\chi(\omega)$ is a frequency dependent term given by

$$\chi(\omega) = \frac{\epsilon_s - \epsilon_\infty}{1 + j\omega t_0} \tag{4}$$

where

- ϵ_∞ is the infinite frequency permittivity
- ϵ_s is the static permittivity
- t_0 is the relaxation time.

Manuscript received June 4, 1991; revised September 23, 1991. This work was supported by Grant CA 44665 from the National Cancer Institute, and by grants for supercomputer time from the Numerical Aerodynamic Simulation Group of NASA and the Supercomputer Center.

The authors are with the Department of Radiation Oncology, Stanford University School of Medicine, Stanford, CA 94305.

IEEE Log Number 9105454.

Substituting (3) and (2) into (1a), and using

$$\boldsymbol{J}(\omega) = \sigma \cdot \boldsymbol{E}(\omega) \tag{5}$$

the following equation is derived

$$j\omega(\epsilon_\infty + \chi(\omega)) \cdot \epsilon_0 \cdot \boldsymbol{E}(\omega) = \nabla \times \boldsymbol{H}(\omega) - \sigma \cdot \boldsymbol{E}(\omega) \tag{6}$$

Moving this equation to the time domain yields

$$\frac{\delta}{\delta t}(\epsilon_0 \cdot \epsilon_\infty \cdot \boldsymbol{E}(t)) + \frac{\delta}{\delta t}\left(\int_0^t \epsilon_0 \cdot \chi(t-\tau) \cdot \boldsymbol{E}(\tau)\, \delta\tau\right) = \nabla \times \boldsymbol{H}(t) - \sigma \cdot \boldsymbol{E}(t) \tag{7}$$

Note that the multiplication of two frequency dependent functions χ and $\boldsymbol{E}$ in the frequency domain in (6) has resulted in a convolution in the time domain. For the sake of simplicity, the rest of the development will be for the case of a 1 dimensional equation, so (7) can be rewritten as

$$\frac{\delta}{\delta t}(\epsilon_0 \cdot \epsilon_\infty \cdot E_y(t, x)) - \frac{\delta}{\delta t}\left(\int_0^t \epsilon_0 \cdot \chi(t-\tau) \cdot E_y(\tau, x)\, \delta\tau\right) = \frac{\delta H_z(t, x)}{\delta x} - \sigma \cdot E_y(t, x). \tag{8}$$

In order to implement the FDTD method, (8) must be written in finite-difference form, a situation which is complicated by the appearance of the convolution integral. However, note that the time domain susceptibility, i.e., the inverse Fourier transform of (4), is

$$\chi(t) = \frac{\epsilon_s - \epsilon_\infty}{t_0} \cdot \exp\left(-\frac{t}{t_0}\right), \qquad \text{for } t > 0. \tag{9}$$

Luebbers, *et al.* [12] have exploited the exponential nature of the susceptibility and rewritten the integral term in (8) as a difference equation:

$$\frac{\delta}{\delta t}\left(\int_0^t \epsilon_0 \cdot \chi(t-\tau) \cdot E_y(\tau, x)\, \delta\tau\right) \approx \epsilon_0 \chi_0(i) \cdot E_y^{n+1}(i) - \epsilon_0 \cdot \sum_{m=0}^{n-1} E_y^{n-m}(i) \cdot \Delta\chi_m(i). \tag{10}$$

Note that $E_y(t, x)$, the continuous time formulation on the left side, corresponds to $E_{n+1}(i)$, the finite difference formulation on the right side with n replacing t as the time variable and i replacing x as the spatial variable, and

$$\chi_0(i) = \int_0^{\Delta t} \chi(\tau, i)\, \delta\tau = (\epsilon_s(i) - \epsilon_\infty(i))\left[1 - \exp\left(-\frac{\Delta t}{t_0}\right)\right] \tag{11}$$

$$\Delta\chi_m(i) = (\epsilon_s(i) - \epsilon_\infty(i)) \cdot \exp\left(-\frac{m \cdot \Delta t}{t_0}\right) \cdot \left[1 - \exp\left(-\frac{\Delta t}{t_0}\right)\right]^2 \tag{12}$$

Details are given clearly in [12] and will not be repeated here.

Rewriting equation 1.a in a finite difference formulation and substituting the results in (10),

$$\epsilon_0\epsilon_\infty(i)\frac{E_y^{n+1}(i) - E_y^n(i)}{\delta t} + \epsilon_0\chi_0(i)E_y^{n+1}(i) - \epsilon_0 \sum_{m=0}^{n-1} E_y^{n-m}(i)\, \Delta\chi_m(i) = \frac{H_z^{n+(1/2)}(i + \tfrac{1}{2}) - H_z^{n+(1/2)}(i - \tfrac{1}{2})}{\delta x} - \frac{\sigma}{2}[E_y^{n+1}(i) + E_y^n(i)] \tag{13}$$

Let ψ represent the convolution term in (10):

$$\psi_y^n(i) = \sum_{m=0}^{n-1} E_y^{n-m}(i)\, \Delta\chi_m(i). \tag{14}$$

Notice that because $\Delta\chi(i)$ in (14) is an exponential, ψ can be determined by the present E value and previous ψ values, which means it will fit the FDTD formulation.

$$\psi_y^n(i) = E_y^n(i)\, \Delta\chi_0(i) + \exp\left(\frac{-\delta t}{t_0}\right)\psi_y^{n-1}(i). \tag{15}$$

Finally, (13) can be rewritten as

$$E_y^{n+1}(i) = ca(i)E_y^n(i) + cb(i) \cdot \left[H_z^{n+(1/2)}(i + \tfrac{1}{2}) - H_z^{n+(1/2)}(i + \tfrac{1}{2})\right] + 2cb(i)\psi_y^n(i) \tag{16}$$

where

$$ca(i) = \frac{\dfrac{\epsilon_\infty}{\epsilon_\infty + \chi_0} - \dfrac{\sigma\delta t}{(\epsilon_\infty + \chi_0)\epsilon_0}}{1 + \dfrac{\sigma\delta t}{(\epsilon_\infty + \chi_0)\epsilon_0}}$$

$$cb(i) = \frac{\frac{1}{2}}{(\epsilon_\infty + \chi_0)\left(1 + \dfrac{\sigma\delta t}{(\epsilon_\infty + \chi_0)\epsilon_0}\right)}. \tag{17}$$

Equations (15) and (16) form the implementation of the FDTD algorithm. In the 3-D formulation, they would be

written as

$$EY(I, J, K) = CAY(I, J, K) * EY(I, J, K) + CBY(I, J, K) * [HZ(I - 1, J, K) - HZ(I, J, K) + HX(I, J, K) - HX(I, J, K - 1)] + 2 * CBY(I, J, K) * PSI(I, J, K) \quad (18a)$$

$$PSI(I, J, K) = EY(I, J, K) * DELCHI(I, J, K) + EXPO * PSI(I, J, K). \quad (18b)$$

CAY and *CBY* are given by (17) for the y direction.

Separate values are calculated for the X and Z directions. The only difference between this and the earlier, "single-frequency" formulation of the FDTD method for biological applications [6], [7], [9], [10] is the last term of (18a), and (18b), which is needed to calculate this term. *DELCHI* is given by (12). *EXPO* is a constant, $\exp(-\Delta t/t_0)$

III. Determining the Parameters

Luebbers *et al.* gave as an example, the calculation of the parameters of water over the range 0 to 80 GHz. This was possible because the dielectric properties of water do not vary rapidly. However, biological tissues like muscle vary substantially with frequency [14], [15]. By limiting calculation to a frequency range of about one decade, it is possible to describe the frequency dependent part of the dielectric properties with a simple one pole susceptibility function similar to (4):

$$\epsilon^*(\omega) = \epsilon_\infty + \frac{\epsilon_s - \epsilon_\infty}{1 + j\omega t_0} + j\frac{\sigma}{\omega\epsilon_0}. \quad (19)$$

The following parameters were used to describe muscle tissue in the frequency range 40 to 433 MHz:

$$\epsilon_\infty = 15$$

$$\epsilon_s = 120$$

$$\sigma = .64 \text{ S/m}$$

$$t_0 = 6.67 \times 10^{-9} \text{ s}.$$

Table I contains the dielectric properties of muscle at the frequencies of interest [14]. Fig. 1 shows a comparison between these values of and the "effective" dielectric constant and conductivity which would result from using the above parameters in the implementation of the $(FD)^2TD$ method described in the previous section. These effective values are calculated from

$$\epsilon_{\text{eff}} = \epsilon_\infty + \text{real}\left\{\frac{\epsilon_s - \epsilon_\infty}{1 + j\omega t_0}\right\}$$

$$\sigma_{\text{eff}} = \sigma - \omega\epsilon_0 \text{ imag}\left\{\frac{\epsilon_s - \epsilon_\infty}{1 + j\omega t_0}\right\} \quad (20)$$

TABLE I
Dielectric Properties of Muscle [14]

Frequency (MHz)	Dielectric Constant	Conductivity
40.68	97.3	0.693
100	71.7	0.889
200	56.5	1.28
300	54	1.37
433	53	1.43

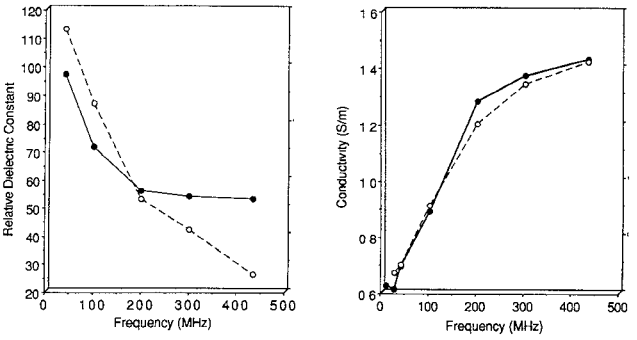

Fig. 1. Comparison of the dielectric properties of muscle as a function of frequency. The solid lines are the tabulated values of Johnson and Guy [14] and the dashed lines are the effective values of the $(FD)^2TD$ method as calculated by (20).

where *real* and *imag* denote the real and imaginary parts, respectively, of the complex quantity. Clearly, the premium was placed on a close match of the conductivity at the expense of the dielectric constant.

IV. Evaluation

In this section the accuracy of a 3-D $(FD)^2TD$ method will be evaluated by comparison against analytic solutions. The specific absorption rate (SAR) is defined as

$$\text{SAR}(i, j, k) = \frac{1}{2}\frac{\sigma(i, j, k)}{\rho} \cdot |E(i, j, k)|^2, \quad (21)$$

where ρ, the density, is assumed to be 1 everywhere. The SAR distribution in a layered sphere illuminated by a plane wave can be calculated by Bessel function expansion [16], [17]. Fig. 2 shows a comparison between the SAR distributions along the major axes in a 20 cm sphere consisting of an outer layer with the dielectric properties half way between air and muscle, and an inner core with the dielectric properties of solid muscle. Results are given at 40, 100, 200, 300, and 433 MHz. The $(FD)^2TD$ values were obtained by one computer run; five separate calculations of the Bessel function expansion were needed. Table II shows the values of the $(FD)^2TD$ parameters used; the Bessel function solutions were computed using the dielectric properties of Johnson and Guy given in Table I.

Correlation between $(FD)^2TD$ and Bessel function data is very good at the lower frequencies, but discrepancies start to show at 300 MHz and are worse at 433 MHz. The reason is easily ascertained from Fig. 1. At 300 and 433 MHz there is a great disparity between the effective di-

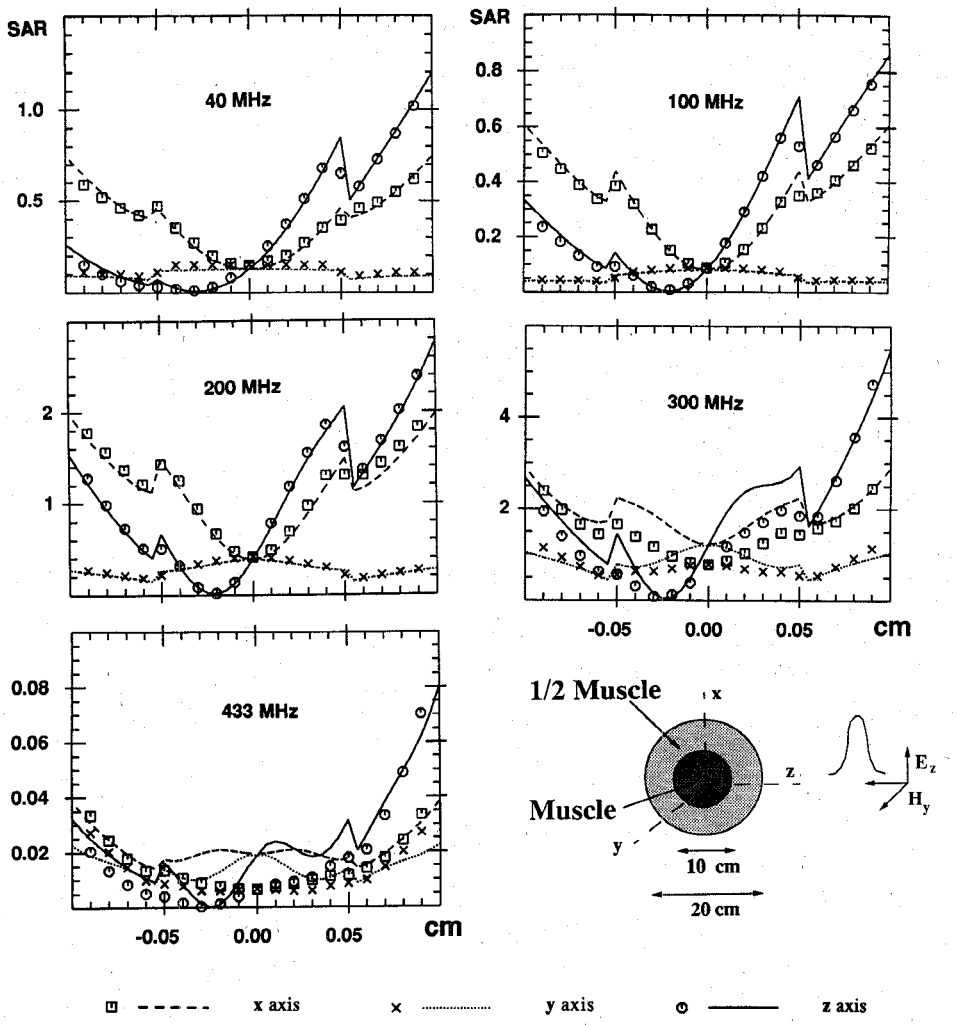

Fig. 2. Comparison of $(FD)^2TD$ and Bessel function solutions for a layered sphere illuminated by a plane wave at 40, 100, 200, 300, and 433 MHz. The inner layer is muscle and the outer layer is half muscle. The $(FD)^2TD$ solutions (icons) were computed using the values in Table II, and the Bessel solutions (lines) used the dielectric properties given in Table I.

TABLE II
PROPERTIES OF THE FREQUENCY-DEPENDENT FDTD METHOD FOR THE FREQUENCY RANGE 40 TO 433 MHz (The RELAXATION TIME IS 0.0067 μs)

Tissue Type	$\epsilon_{infinity}$	ϵ_s	σ
Muscle	15	120	0.64
1/2 Muscle	7.8	60	0.32
Fat	1.5	12	0.07

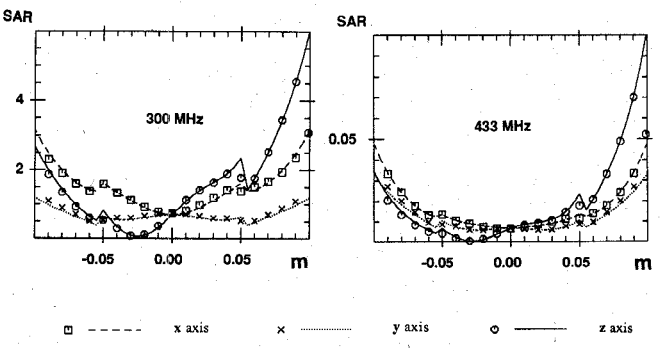

Fig. 3. Comparison of $(FD)^2TD$ and Bessel function solutions for a layered sphere illuminated by a plane wave at 300 and 433 MHz. The inner layer is muscle and the outer layer is half muscle. The $(FD)^2TD$ solutions (icons) were computed using the values in Table II, and the Bessel solutions (lines) used the dielectric properties computed by equation 20 and graphed in Fig. 1.

electric constant and the actual one used for the Bessel solution. If the Bessel solutions are rerun using the effective values, i.e., $\epsilon = 42$ and $\sigma = 1.34$ at 300 MHz, and $\epsilon = 26$ and $\sigma = 1.42$ at 433 MHz, agreement is much better (Fig. 3). Obviously, it is the inability of (19) to adequately cover the higher frequencies which lead to the discrepancies in Fig. 2.

In contrast, it is interesting to look at the errors when one set of parameters is used with a multiple frequency FDTD method which does *not* take into account the frequency dependence of the tissues. Fig. 4 is a comparison of FDTD values and Bessel solutions using $\epsilon = 72$ and $\sigma = 0.89$, the values at 100 MHz. At 40 MHz, agreement is quite good. However, at 200 MHz there are substantial alterations in the pattern, and by 433, it has changed completely!

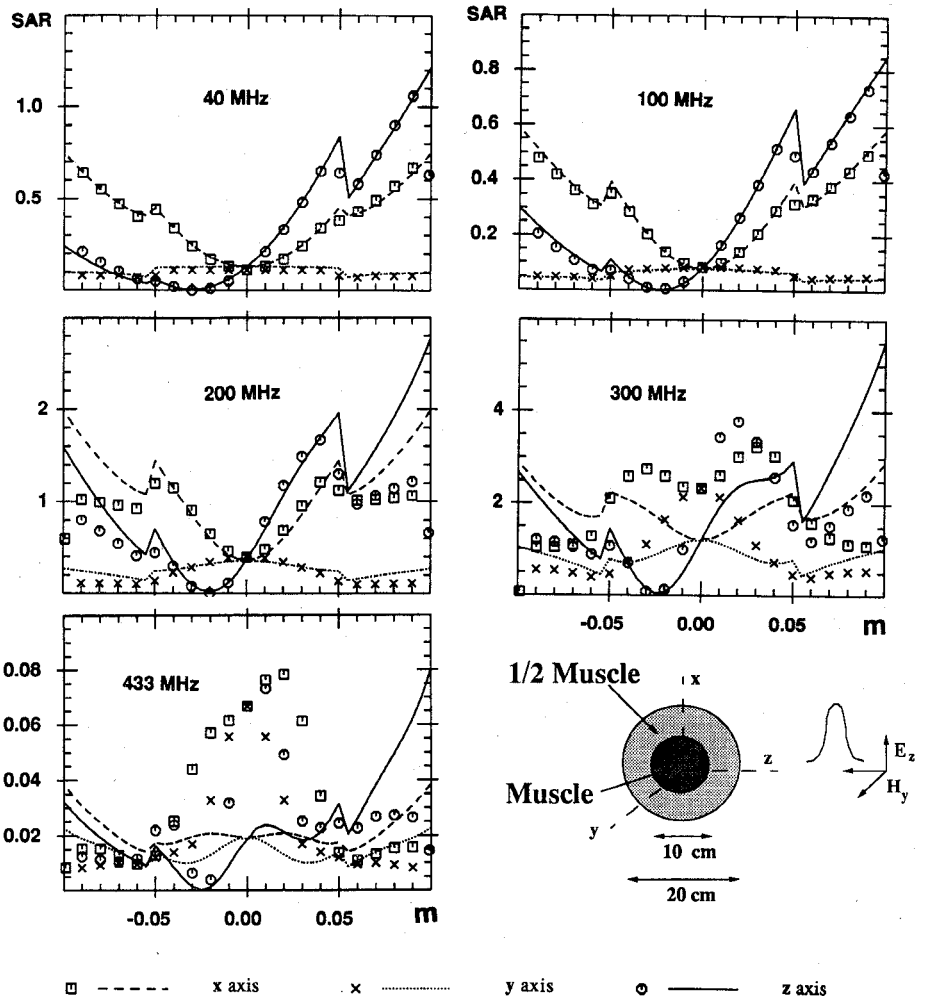

Fig. 4. Comparison of the conventional FDTD method and Bessel function solutions for a layered sphere illuminated by a plane wave at 40, 100, 200, 300, and 433 MHz. The inner layer is muscle and the outer layer is half muscle. The FDTD solutions (icons) were computed using the dielectric properties of muscle and half muscle at 100 MHz; the Bessel solutions (lines) were computed using the frequency dependent values for muscle in Table I.

Fig. 5 is a comparison using a three layered sphere consisting of an outer muscle layer, an inner fat layer between 4 and 7 cm, and an inner muscle core. The dispersive FDTD method is capable of following the abrupt changes offered by this problem. Again, at the higher frequencies, some discrepancy starts to show.

V. An Example in Hyperthermia Applicator Design

The use of the FDTD method to determine the SAR distribution of a biological body in the near field of an RF antenna has been demonstrated [9]. It was shown that the FDTD method could play a role in developing new applicators for deep regional hyperthermia by being able to accurately predict the SAR pattern in a muscle/fat phantom. It was further shown that the same program could predict the energy deposition in a patient being treated by such applicators, enabling the evaluation of the usefulness of potential applicators and their comparison with commercially available equipment. Of course, using the conventional FDTD method, the each simulation only gave the answer at one frequency.

In this section the use of the $(FD)^2TD$ to predict the wide-band SAR distributions for discrete RF hyperthermia applicators will be demonstrated. This will be done by modeling an applicator and then simulating the treatment of a cancer patient using two such applicators. Fig. 6 is a diagram of the applicator. The antenna is a metal dipole in a configuration known as a "bow tie" antenna. The bow tie antenna is used because it has a relatively wide bandwidth. It is contained in a clear plastic housing filed with distilled water to facilitate coupling to a human body. (This applicator has not been constructed. This is merely an example of the type of applicator a designer might try.) Fig. 7 is a diagram of how two such applicators might be used to treat a large eccentric tumor next to the lung. A full three dimensional model of the applicators and the patient was created [9], [10], [18], using a cell size of 1 cm and a time step of 0.0167 ns. This required 50 slices of the patient's CT scan. The program to simulate such a configuration requires a problem space of

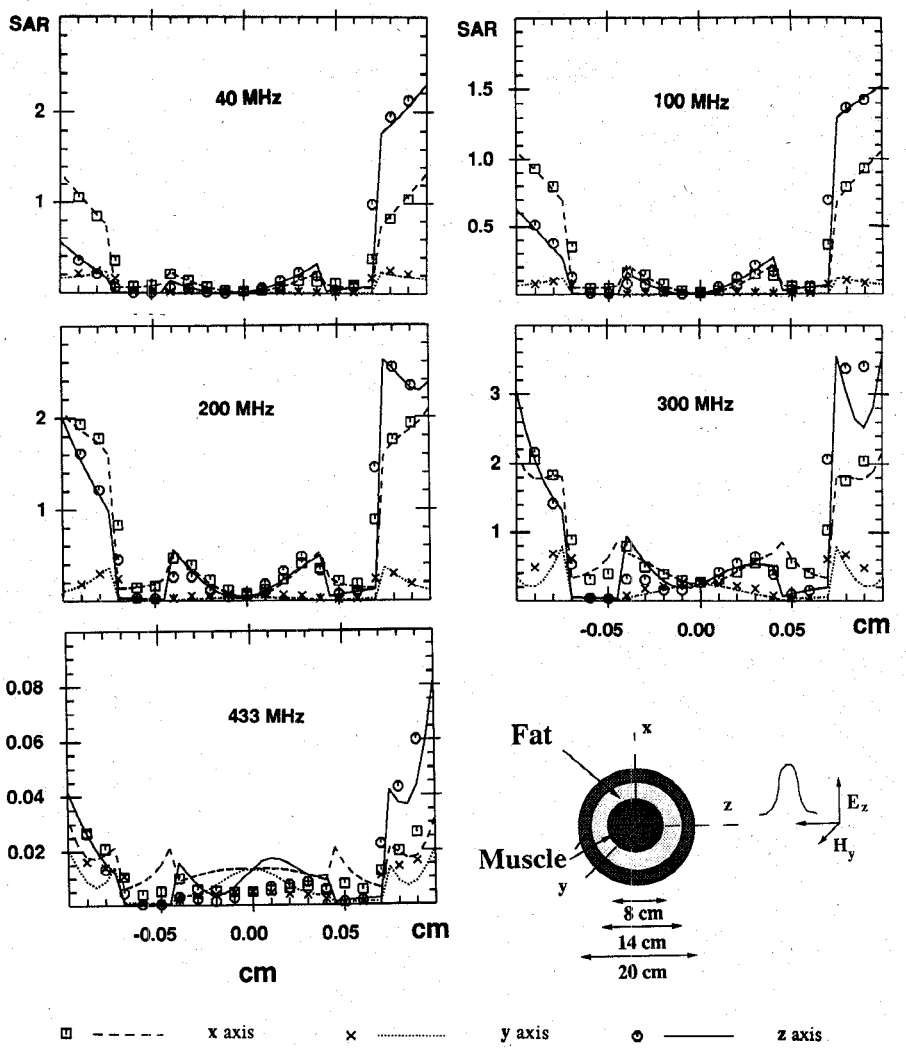

Fig. 5. Comparison of $(FD)^2TD$ and Bessel function solutions for a layered sphere illuminated by a plane wave at 40, 100, 200, 300, and 433 MHz. The inner and outer layers are muscle and the middle layer is fat. The $(FD)^2TD$ solutions (icons) were computed using the values in Table II, and the Bessel solutions (lines) used the dielectric properties given in Table I.

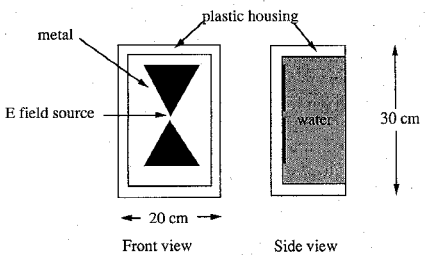

Fig. 6. Possible broad band applicator for deep regional hyperthermia.

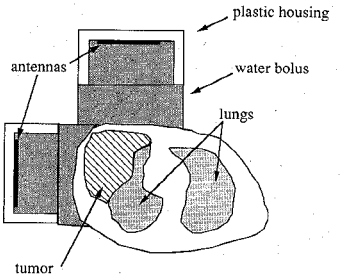

Fig. 7. Diagram of simulated hyperthermia treatment configuration using two applicators.

$60 \times 78 \times 78 = 371\,040$ cells, and requires 2000 time steps to converge. It takes about 10 megawords of core memory and runs in about 200 CPU seconds using a Cray YMP supercomputer. Two such runs, corresponding to the two applicators are made, and the SAR is calculated from the superposition of the E fields from the two applicators. (This technique, as it is used for fixed position applicators, is described in detail in [10].) Fig. 8 shows the SAR pattern for 40, 70, 100, 140, and 200 MHz, displayed as iso-SAR patterns over the patient's CT scans. Each contour represents 10% of maximum SAR. (Normally the iso-contours are color coded. Thirty such slices with the iso-SARs displayed over them are available and the operator can access them by clicking the mouse. This is described in [18].) Regrettably, seeing only one slice of the SAR values does not tell the whole tale. Other slices, above and below the one being shown, contain substantial "hot spots," corresponding to normal E-fields

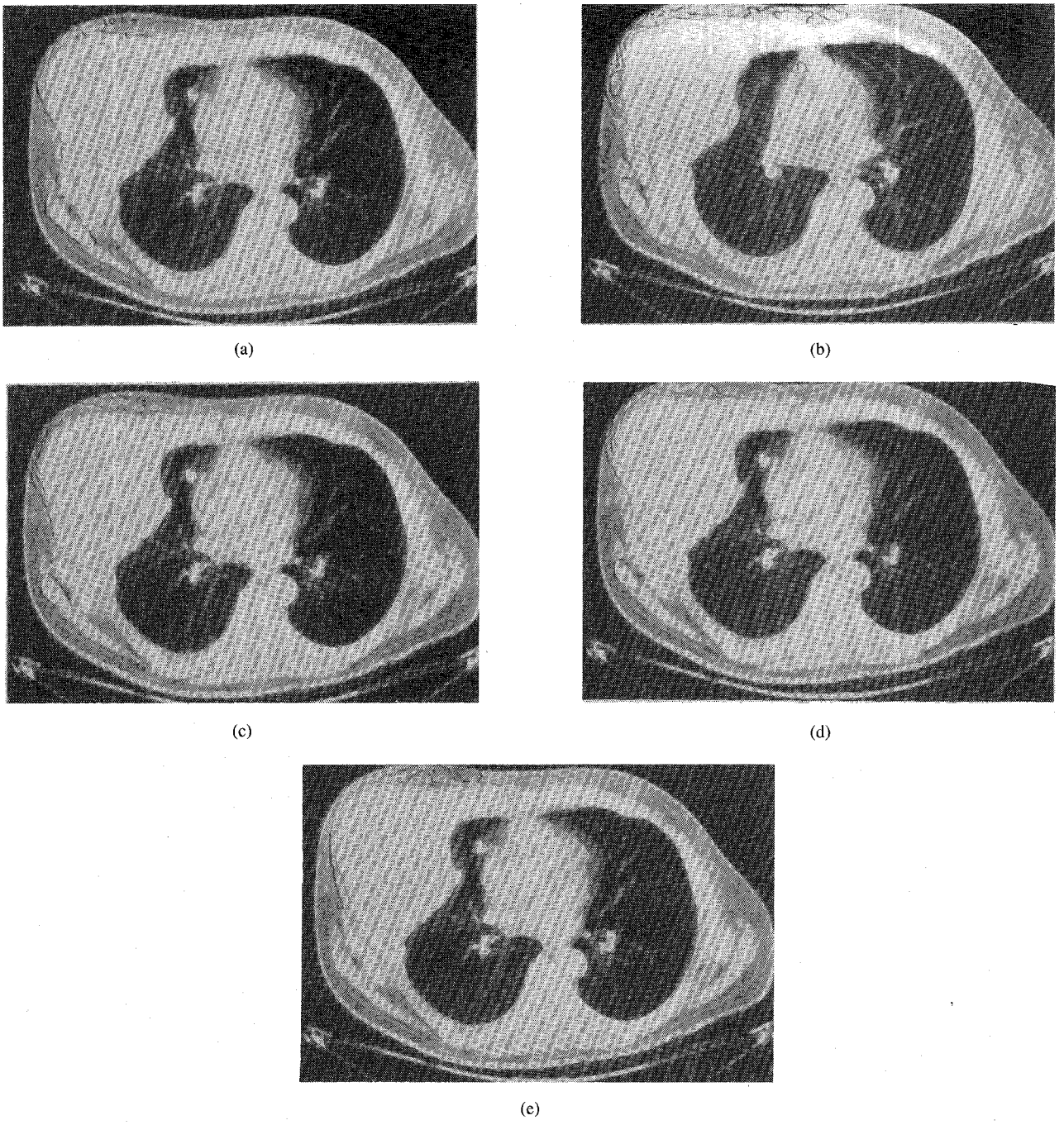

Fig. 8. Simulated results of the hyperthermia treatment configuration in Fig. 7 at (a) 40 MHz, (b) 70 MHz, (c) 100 MHz, (d) 140 MHz, and (e) 200 MHz. Each contour represents 10% of maximum SAR throughout the entire 3-D region.

generated by the ends of the antennas. Note that some slices, even though they seem to show a good energy deposition pattern in the tumor, only have 4 or 5 contours, i.e., 40 or 50% of maximum. Conclusion: this applicator would be wholly inadequate for deep regional hyperthermia.

Discussion

The implementation of the frequency-dependent finite-difference time-domain $(FD)^2TD$ method for biological applications has been described. This makes possible multiple frequency information from one computer run because it allows for the frequency dependence of the tissue properties. By making a comparison of SAR distributions in layered spheres illuminated by a plane wave, the accuracy of this method was shown to be very good over the frequency range 40 to 200 MHz. It is likely that the frequency range of this accuracy is limited only by the one pole susceptibility function given in (4). A more elaborate formulation of the method would probably lead to a broader frequency range.

To illustrate the usefulness of this method, a hyperthermia treatment with a broad band applicator was sim-

ulated. Only two computer runs, one for each applicator, were needed to predict the SAR distribution in a cancer patient at 40, 70, 100, 140, and 200 MHz. Such a method not only aids in the design of new applicators, but also allows comparison of their effectiveness with commercially available equipment.

The method has similar potential use in the field of EM dosimetry where it is necessary to determine SAR distribution for health and safety reasons. Substantially more information is available when the SAR distribution can be obtained over a large frequency range with one computer run rather than making separate runs for every frequency of interest.

Acknowledgment

The author is extremely grateful to Dr. D. Borup of Technoscan, Inc., Salt Lake City, Utah for the Bessel routines used in this paper, and to Dr. J. Deford of Lawrence Livermore National Laboratory for many helpful discussions.

References

[1] K. S. Yee, "Numerical solution of initial boundary value problems involving Maxwell's equations in isotropic media," *IEEE Trans. Antennas Propagat.*, vol. AP-17, pp. 585–589, 1966.

[2] A. Taflove, "Review of the formulation and applications of the finite-difference time-domain method for numerical modeling of electromagnetic wave interactions with arbitrary structures," *Wave Motion*, vol. 10, pp. 547–582, Dec. 1988.

[3] K. Umashankar and A. Taflove, "A novel method to analyze electromagnetic scattering of complex objects," *IEEE Trans. Electromagn. Compat.*, vol. EMC-24, pp. 397–405, 1982.

[4] A. Taflove and K. Umashankar, "Radar cross section of general three-dimensional scatterers," *IEEE Trans. Electromagn. Compat.*, vol. EMC-25, pp. 433–439, 1983.

[5] A. Taflove, "Application of the finite-difference time-domain method to sinusoidal steady-state electromagnetic penetration problems," *IEEE Trans. Electromagn. Compat.*, vol. EMC-22, pp. 191–202, 1980.

[6] D. M. Sullivan, D. T. Borup, and O. P. Gandhi, "Use of the finite-difference time-domain method in calculating EM absorption in human tissues," *IEEE Trans. Biomed. Eng.*, vol. BME-34, pp. 148–157, Feb. 1987.

[7] ——, "Use of the finite-difference time-domain method for calculating EM absorption in man models," *IEEE Trans. Biomed. Eng.*, vol. 35, pp. 179–185, Mar. 1988.

[8] C. W. Wang and O. P. Gandhi, "Numerical simulation of annular phased arrays for anatomically based models using the FDTD Method," *IEEE Trans. Microwave Theory Tech.*, vol. 37, pp. 118–126, Jan. 1989.

[9] D. M. Sullivan, "Three-dimensional computer simulation in deep regional hyperthermia using the FDTD method," *IEEE Trans. Microwave Theory Tech.*, vol. 38, pp. 204–211, Feb. 1990.

[10] ——, "Mathematical methods for treatment planning in deep regional hyperthermia, *IEEE Trans. Microwave Theory Tech.*, vol. 39, pp. 864–872, May 1991.

[11] C. M. Furse, S. P. Mathur, and O. P. Gandhi, "Improvements to the finite-difference time-domain method for calculating the radar cross section of a perfectly conducting target," *IEEE Trans. Microwave Theory Tech.*, vol. 38, pp. 919–927, July 1990.

[12] R. Luebbers *et al.*, "A frequency-dependent finite-difference time-domain formulation for dispersive materials," *IEEE Trans. on Electromagn. Compat.*, vol. 32, pp. 222–227, Aug. 1990.

[13] ——, "A frequency-dependent finite-difference time-domain formulation for transient propagation in plasma," *IEEE Trans. Antennas Propagat.*, vol. 39, pp. 29–34, Jan. 1991.

[14] C. C. Johnson and A. W. Guy, "Nonionizing electromagnetic wave effects in biological materials and systems," *Proc. IEEE*, vol. 60, pp. 692–718, June 1972.

[15] M. A. Stuchly and S. S. Stuchly, "Dielectric properties of biological substances—tabulated," *J. Microwave Power*, vol. 15, pp. 19–26, 1980.

[16] J. A. Stratton, *Electromagnetic Theory*, New York: McGraw-Hill, 1941.

[17] J. R. Mautz, "Mie series solution for a sphere," *IEEE Trans. Microwave Theory Tech.*, vol. MTT-26, p. 375, 1978.

[18] B. J. James and D. M. Sullivan, "Direct use of CT scans for hyperthermia and radiation therapy treatment planning," *IEEE Trans. Biomed. Eng.*, accepted for publication.

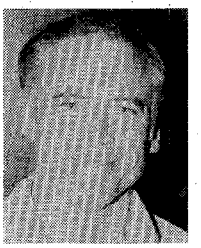

Dennis Sullivan (M'89) received the B.S. degree in electrical engineering from the University of Illinois in 1973. He later entered the University of Utah as a double major in electrical engineering and ballet. With the encouragement of the ballet faculty, he completed his Ph.D. degree in electrical engineering in 1987.

He is presently a Research Engineer at the Department of Radiation Oncology at the Stanford University School of Medicine. His interests are computer simulation for cancer treatment.